Colloids and Surfaces B: Biointerfaces 87 (2011) 236–242

Contents lists available at ScienceDirect

Colloids and Surfaces B: Biointerfaces

journal homepage: www.elsevier.com/locate/colsurfb

Dead Sea Minerals loaded polymeric nanoparticles

Alberto Dessy[a], Stephan Kubowicz[b], Michele Alderighi[a], Cristina Bartoli[a], Anna Maria Piras[a], Ruth Schmid[b], Federica Chiellini[a,*]

[a] Laboratory of Bioactive Polymeric Materials for Biomedical and Environmental Applications (BIOlab), UdR INSTM, Department of Chemistry & Industrial Chemistry, University of Pisa, Pisa, Italy
[b] SINTEF Materials and Chemistry, Synthesis and Properties, Polymer Particles and Surface Chemistry, Postboks 4760 Sluppen, NO-7465 Trondheim, Norway

ARTICLE INFO

Article history:
Received 26 January 2011
Received in revised form 19 April 2011
Accepted 15 May 2011
Available online 20 May 2011

Keywords:
Polymeric nanoparticles
Dead Sea Minerals
Psoriasis
Skin diseases
Bioerodible polymer
Miniemulsion

ABSTRACT

Therapeutic properties of Dead Sea Water (DSW) in the treatment of skin diseases such as atopic dermatitis, psoriasis and photo aging UV damaged skin have been well established. DSW is in fact rich in minerals such as calcium, magnesium, sodium, potassium, zinc and strontium which are known to exploit anti-inflammatory effects and to promote skin barrier recovery.

In order to develop a Dead Sea Minerals (DSM) based drug delivery system for topical therapy of skin diseases, polymeric nanoparticles based on Poly (maleic anhydride-alt-butyl vinyl ether) 5% grafted with monomethoxy poly(ethyleneglycol) 2000 MW (PEG) and 95% grafted with 2-methoxyethanol (VAM41-PEG) loaded with DSM were prepared by means of a combined miniemulsion/solvent evaporation process. The resulting nanoparticles were characterized in terms of dimension, morphology, biocompatibility, salt content and release. Cytocompatible spherical nanoparticles possessing an average diameter of about 300 nm, a time controlled drug release profile and a high formulation yield were obtained.

1. Introduction

Psoriasis and atopic dermatitis represent the most common skin diseases found in the entire population. Different factors seem to be related both to atopic dermatitis and psoriasis leading the scientific community to consider them as "complex diseases" [1].

Both psoriasis and atopic dermatitis are characterized by the infiltration of inflammatory cells into the dermis and epidermis which causes the hyper-proliferation of keratinocytes in psoriatic patients and the formation of inflamed patches in patients with atopic dermatitis [2]. The inflammatory cells involved in the over mentioned processes are different in the two pathologies. While in psoriasis inflammatory cells invading the skin are TH1 cells, macrophages, dendridic cells and neutrophils, in atopic dermatitis TH2 cells, eosinophil and mast cells invade the skin [3]. In both psoriasis and atopic dermatitis alterations regarding skin properties are present; for instance, the skin of patients with atopic dermatitis demonstrates increased transepidermal water loss (TEWL) [4] and skin barrier function alterations, which are also observed in psoriatic skin [5–9].

Similar disorders can also be observed in UV-damaged healthy skin. Prolonged UV-light exposure can in fact lead to acute responses including erythema, keratinocytes hyper-proliferation and skin permeability barrier alterations [10].

In the treatment of skin diseases, the beneficial effects of Dead Sea Water (DSW) are well known [11–13]. Therapeutic baths in the Dead Sea are commonly used as a treatment both for psoriasis, atopic dermatitis and UV-damaged skin [14]. DSW salt composition is represented by a high concentration of different minerals such as magnesium, calcium, bromide, sodium, potassium, zinc and strontium [15,16].

Although the exact mechanism of DSW skin beneficial effects is still not well understood, the above mentioned minerals, whose penetration through psoriatic skin is more profound than in healthy skin, are known to bring about anti-inflammatory effects and to promote skin barrier recovery [17]; moreover bromide is known to have a strong inhibitory effect on fibroblast proliferation, while magnesium is implicated in the regulation of cyclic adenosine 3′–5′ monophosphate and cyclic guanosine 3′–5′ monophosphate levels which, altered in psoriatic tissue, determine the excessive keratinocyte proliferation [18].

In recent years, miniemulsions have been studied and successfully applied in cosmetics and therapeutics for skin treatments. They can be defined as heterophase systems consisting of thermodynamically stable nanodroplets (possessing an average diameter between 50 and 500 nm) in a continuous phase [19]. Miniemulsions can be basically divided into oil-in-water (O/W)

* Corresponding author at: BIOLab, Department Chemistry & Ind. Chemistry, University of Pisa, Via Vecchia Livornese 1291, San Piero a Grado (Pisa) Italy.
Tel.: +39 050 2210305; fax: +39 050 23210332.
E-mail address: federica@dcci.unipi.it (F. Chiellini).

0927-7765/$ – see front matter © 2011 Elsevier B.V. All rights reserved.
doi:10.1016/j.colsurfb.2011.05.024

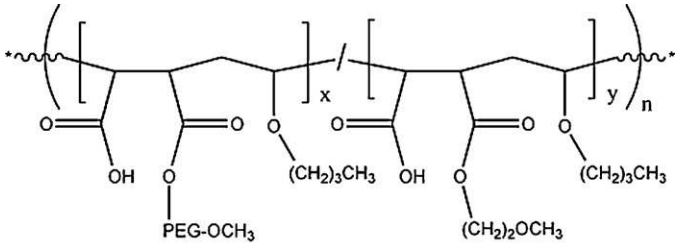

VAM41-PEG

Fig. 1. Chemical structure of VAM41-PEG.

and water-in-oil systems (W/O); the above mentioned systems are commonly studied both in the development of miniemulsion polymerization processes [20,21] and for the production of emulsion-based drug delivery systems for the time-controlled administration of antitumor agents, peptide drugs, sympatholytics, local anaesthetics, steroids, anxiolytics, anti-infective drugs, vitamins, anti-inflammatory drugs and dermatological products [22]. The use of miniemulsions in the development of skin care products presents many advantages related to the system stability against sedimentation [23] and to the use of skin-friendly ingredients [24]. In the present work, the scientific background related to the preparation of miniemulsions for skin treatments was transferred to the preparation of solid nanoparticles based on Poly (maleic anhydride-alt-butyl vinyl ether) 5% grafted with m-PEG (2000) and 95% grafted with 2-methoxyethanol (VAM41-PEG), loaded with Dead Sea Minerals (DSM). The particles were finally dispersed in cosmetic oil to allow the topical administration and to favour a drug controlled release and penetration through the skin barrier [25]. The oil is in fact expected to penetrate into the skin, transporting particles into the epidermis, where DSM may be released thanks to skin moisture. The use of a polymeric nanoparticle based system, besides offering a longer life-time if compared to water-in-oil emulsions, can also permit the addition of dermal drugs such as Cyclosporins, Retinoids and Corticosteroids to the formulation without altering its stability.

2. Materials and methods

2.1. Materials

VAM41-PEG: Poly (maleic anhydride-alt-butyl vinyl ether) 5% grafted with monomethoxy poly(ethyleneglycol) 2000 MW and 95% grafted with 2-methoxyethanol (Fig. 1) was synthesized at Biolab, Department of Chemistry and Industrial Chemistry, University of Pisa [26].

Spectra/Por dialysis membranes of regenerated cellulose (MWCO: 15000 Da) were purchased from Spectrum Labs.

Paraffin oil (Norpar 12) was purchased from Exxon Mobil; Dimethylaminopyridine (DMAP), Poly(ethylene glycol) [M.W. 2000] (PEG2000), 2-Methoxyethanol, Almond Oil, Ethanol and Diethyl Ether were purchased from Sigma Aldrich; Hypermer B246-E, Span 80, Nonylphenol Ethoxylate and Brij 72 were supplied by Uniqema; Styrene-divinyl benzene sulfonic resin (Amberlyst 15, 4.6 meq g^{-1} exchange capacity) was supplied by Fluka; Ethanol and Tetrahydrofuran (THF) were purchased by Carlo Erba; Poly[(maleic anhydride)-alt-(butylvinyl ether)] polymer was supplied by Polymer Laboratories; Cell line 3T3/BALB-C Clone A31 mouse embryo fibroblast (CCL163) was purchased from American Type Culture Collection (ATCC) and propagated as indicated by the supplier; Dulbecco's Modified Eagles Medium (DMEM), 0.01 M pH 7.4 phosphate buffer saline without Ca^{2+} and Mg^{2+} (PBS), bovine calf serum (BCS), glutamine and antibiotics (penicillin/streptomycin) were purchased from GIBCO/Brl; Cell proliferation reagent WST-1 was provided by Roche diagnostic.

Table 1
List of nanoparticle formulations and the corresponding DSW dilutions applied in their preparation.

Formulation name	% of DSW in the aqueous solution (v/v)	DSM content% (w/v)
Nps_Dsw_0	–	–
Nps_Dsw_1/2[A]	8	1
Nps_Dsw_[A]	16	2
Nps_Dsw_2[A]	32	4

Dead Sea Water (DSW) was kindly supplied by Ahava-Dead Sea Laboratories (Israel), with the following chemical composition: Ca^{2+} 36–40 g/l, Cl^- 320–370 g/l, Mg^{2+} 90–95 g/l, K^+ 1.3–1.5 g/l, Na^+ 1.5–2.5 g/l, Br^- 11–12 g/l, Sr^{2+} 0.75–0.85 g/l.

The commercial products were used without any preliminary purification if not otherwise stated.

2.2. Methods

2.2.1. VAM41-PEG synthesis

VAM41-PEG was synthesized as previously reported [26]. Briefly, 2.00 g of Poly[(maleic anhydride)-alt-(butylvinyl ether)] (10 mmol of maleic anhydride units), 1.01 g m-PEG (0.5 mmol) and 0.058 g DMAP were dissolved in 80 ml of anhydrous THF under nitrogen atmosphere. The resulting solution was maintained at 75 °C and monitored by IR spectroscopy. After 24 h, when the intensity of the anhydride C=O band at 1786 cm^{-1} reached a constant intensity, 7.71 g 2-methoxyethanol (100 mmol) were added and the solution was maintained at 75 °C under stirring until the anhydride C=O band disappeared (24 h). The solution was then cooled to room temperature and added to a mixture of 50/50 (v/v) diethyl ether/petroleum ether (volume ratio 1/10) with vigorous stirring. The resulting pink precipitate was dried under high vacuum to constant weight. The removal of excess DMAP was performed by ion exchange chromatography. The polymer was dissolved in ethanol (EtOH)/H_2O (80/20, v/v) and loaded on Amberlyst 15 exchange resin, previously conditioned with H_2O, H_2O/EtOH (80/20, v/v), H_2O/EtOH (50/50, v/v), and finally with H_2O/EtOH (20/80, v/v). The solution collected at the end of the column was dried under high vacuum to constant weight. The polymer was then characterized by means of FT-IR and ^1H NMR spectra analysis.

FT-IR (KBr): 3500–3300 (COOH), 1735 (C=O ester), 1715 (C=O acid), 1210–1160 and 1095 cm^{-1} (ester). ^1H NMR (DMSO-d_6): δ = 12.4 (COOH), 4.3–3.8 (CH_2OCO), 3.8–3.3 ($OCH_2CH_2O + CHOCH_2 + CH_2OCH_3$), 3.3–3.1 ($CH_3O$), 3.1–2.3 (OCCHCHCO), 2.3–1.6 (CH_2CH), 1.6–1.0 ($CH_2CH_2CH_3$), 1.0–0.6 (CH_2CH_3).

2.2.2. Nanoparticle formulation

DSM loaded polymeric nanoparticles were prepared by means of a water-in-oil (W/O) combined miniemulsion/solvent evaporation process. 50 mg of VAM41-PEG were dissolved in 1 ml of ethanol and after polymer dissolution 0.5 ml of an aqueous dilution of DSW was added under magnetic stirring. Four different formulations were tested, differing in the dilution of DSW used in the preparation of the nanoparticles. Table 1 reports the applied DSW dilutions and the corresponding DSM concentrations.

In parallel, 87.5 mg of Hypermer B246-E were dissolved in 3.5 ml of Norpar 12 by heating to 37 °C on a hot plate/magnetic stirrer. Hypermer B246-E is an A-B-A block copolymer surfactant; the lipophilic A chains consist of polyhydroxystearic acid and the B hydrophilic part is polyethylene glycol.

The aqueous polymeric solution was then added to the oil solution and maintained under vigorous magnetic stirring for

approximately 1 min. The resulting emulsion was sonicated at 200 W for 1 min using a Labsonic 2000 ultrasonifier.

The resulting nanoemulsions were treated in a Büchi EL131 Rotavapor apparatus, equipped with a Vacuubrand CVC2 membrane pump (40 °C, 70 mbar), for 2 h to remove ethanol and water. The polymeric nanoparticles were then centrifuged at 3000 rpm for 10 min using a Sigma 3E-1 centrifuge. The resulting pellet was dispersed in 10 ml of diethyl ether and centrifuged again at 3000 rpm for 10 min to remove excess surfactant. The purified nanoparticles were dried under high vacuum, at room temperature, until constant weight.

The formulation yield was calculated as the ratio between the dry weight of the centrifuged pellet and the sum of the starting weight of each component.

$$\text{Formulation yield} = \frac{\text{Nanoparticles (g)}}{\text{Formulation components (g)}} \times 100 \quad (1)$$

All nanoparticle formulations were prepared in triplicates.

2.2.3. Nanoparticle suspension in almond oil

5 mg of purified nanoparticles were dispersed in 4 ml of diethyl ether and 4 ml of almond oil were added under magnetic stirring. The system was maintained over night in a water bath (40 °C) to let the ether evaporate.

2.2.4. Nanoparticle salt content determination

20 mg of purified nanoparticles were suspended in 5 ml of deionised water. In order to dissolve the nanoparticles, 10 μl of NaOH 1 N were added under magnetic stirring. After dissolution, the solution was put in a dialysis tube (regenerated cellulose, 15 kDa MWCO) using 600 ml of deionised water as outer phase. Conductivity of the external medium was measured using a Mettler Toledo conductivity meter SG3 equipped with conductivity sensor InLab 737. A blank experiment was carried out separately by putting 10 μl of NaOH 1 N and 5 ml of water into a dialysis tube; the conductivity of the external medium was measured. Salt concentration was estimated by using a calibration curve obtained by plotting conductivity values of aqueous DSM solutions (7–42 μg/ml) *vs.* their concentration in μg/ml (R^2 = 0.9999).

The nanoparticle salt content was expressed in terms of encapsulation efficiency (E.E.; Eq. (2)) and salt loading (Ldg; Eq. (3)).

$$\text{E.E.} = \frac{\text{Salts loaded (g)}}{\text{Total salts (g)}} \times 100 \quad (2)$$

$$\text{Ldg} = \frac{\text{Salts loaded (g)}}{\text{Nanoparticles (g)}} \times 100 \quad (3)$$

The nanoparticle salt content was calculated as the mean value of at least 3 replicates for each nanoparticle formulation.

2.2.5. Nanoparticle salt release kinetic

The salt release kinetic of the nanoparticles was analyzed by suspending 3 mg of purified nanoparticles in 1 ml of almond oil. The resulting suspension was put on top of deionised water (30 ml), using a separation funnel as a container. The water phase was stirred mildly, while mixing with the upper oil phase was avoided. Water samples were collected periodically and conductivity measurements were carried out. A blank experiment was carried out by putting a known volume of pure almond oil on top of water, using the same experimental setup. Salt concentration was estimated by using a calibration curve obtained by plotting conductivity values of aqueous DSM solutions (7–42 μg/ml) *vs.* their concentration in μg/ml (R^2 = 0.9999). All samples were assayed in triplicates.

2.2.6. Nanoparticle characterization

Dimensional analyses were carried out by means of a Malvern Zetasizer Nano ZS. Nanoparticle suspensions were added into a glass cuvette and almond oil was used as background. Three runs were performed on each sample.

Nanoparticle morphology was investigated by means of Scanning Electron Microscopy (SEM) and Atomic Force Microscopy (AFM). SEM and AFM samples were prepared from dry, purified nanoparticles. Gold sputtering was performed before SEM analysis. A commercial AFM instrument (Multimode microscope working with a Nanoscope IV controller, Veeco Instr. Santa Barbara Ca., USA) operated in tapping mode was used to evaluate the surface topography of the nanoparticles, which were deposited on a freshly cleaved surface of mica.

2.2.7. Infrared spectroscopy (IR)

IR spectra analysis was performed on cast films on disposable polytetrafluoroethylene (19-mm aperture) IR cards, by using a Perkin-Elmer System One FTIR-Spectrometer. IR spectra analyses were recorded for DSM, Hypermer B246-E, VAM41-PEG and the water samples from the release kinetic experiments with Nps_Dsm_½[A], Nps_Dsm_2[A] and Nps_Dsm_ [A].

2.2.8. Nuclear magnetic resonance spectroscopy (NMR)

NMR spectra were recorded on a Varian Gemini 200 spectrometer using a Sparc 4 (Sun) console and VNMR 6.1B software. Spectra were processed by using MacFID 1D 5.3 (Tecmag) software. NMR spectra were recorded in 5–10% (w/v) solutions in deuterated solvents at 25 °C, with tetramethylsilane (TMS) as internal standard. ^{1}H NMR spectra were recorded at 200 MHz, using the following spectral conditions: 3 kHz spectral width, 30° impulse, 2 s acquisition time, 16 transients.

2.2.9. Cytotoxicity tests

Cytotoxicity evaluation of DSM loaded nanoparticles was carried out using the 3T3/BALB-C Clone A31 cell line. Cells were grown in DMEM containing 10% (v/v) Bovine Calf Serum, 4 mM glutamine, 100 U/ml of penicillin and 100 μg/ml of streptomycin.

Subculturing: A 25 ml flask containing exponentially growing 3T3 cells was observed under an inverted microscope for cell confluence. DMEM was then removed completely, and cells were rinsed for a few minutes with PBS. The buffer solution was removed, and cells were incubated with 0.5 ml of trypsin/EDTA solution at 37 °C in a 5% CO_2 incubator for 5 min or until the monolayer started to detach from the flask. Cells were suspended in an appropriate volume of DMEM at a split ratio of 1:6 or 1:10 in a 75 ml flask.

For the determination of the cytocompatibility of DSM loaded VAM41-PEG based nanoparticles, a subconfluent monolayer of 3T3 fibroblasts was trypsinized using a 0.25% trypsin, 1 mM EDTA solution, centrifuged at 200 × *g* for 5 min, re-suspended in growth medium and counted. Appropriate dilution was made in order to obtain 3×10^3 cells per 100 μl of medium, the final volume present in each well of a 96 well plate. Cells were incubated at 37 °C, 5% CO_2 for 24 h until 60–70% confluence was reached. The medium from each well was then removed and replaced with medium containing different nanoparticle concentrations. Nanoparticle suspensions in cell medium were achieved by adding a known amount of dry, purified nanoparticles to a known volume of DMEM; the suspension was then sonicated with a Vibra-Cell sonicator (Vc 130) for 60 s at 20 kHz and 20% of amplitude. After a homogeneous suspension was obtained, 10% (v/v) Bovine Calf Serum, 4 mM glutamine and 100 U/ml:100 μg/ml penicillin:streptomycin were added to the suspension. Control cells were incubated with fresh growth medium sonicated for 60 s at 20 kHz and 20% of amplitude. After 24 h of incubation with medium containing DSM loaded nanoparticles, cells were analyzed for viability with Cell Proliferation Reagent WST-1. Cells were incubated with WST-1 reagent diluted 1:10 (as indicated by the manufacturer) for 4 h at 37 °C, 5% CO_2. Plates were then analyzed with a Biorad Microplate Reader. Measurements of

Table 2
Formulation Yields.

Formulation name	Formulation yield (% ± S.D.)
Nps_Dsm_0	0
Nps_Dsm_½[A]	47 ± 2.1
Nps_Dsm_[A]	58.5 ± 3
Nps_Dsm_2[A]	80 ± 2.5

Table 3
Polymeric nanoparticles diameter distribution.

Formulation name	Nanoparticles diameter distribution (nm ± S.D.)
Nps_Dsm_0	0
Nps_Dsm_½[A]	226 ± 15
Nps_Dsm_[A]	342 ± 32
Nps_Dsm_2[A]	303 ± 26

Table 4
Nanoparticles DSM loading and encapsulation efficiency (values estimated within an instrumental error of 3%).

Formulation	Loading (% ± S.D.)	E.E. (% ± S.D.)
Nps_Dsm_½[A]	8 ± 1	15 ± 0.8
Nps_Dsm_[A]	11.5 ± 1.2	19.3 ± 0.9
Nps_Dsm_2[A]	8.5 ± 1.9	16 ± 1.5

formazan dye absorbance were carried out at 450 nm, with the reference wavelength at 620 nm.

3. Results and discussion

3.1. DSM loaded polymeric nanoparticles

Poly (maleic anhydride-alt-butyl vinyl ether) 5% grafted with m-PEG (2000) and 95% grafted with 2-methoxyethanol (VAM41-PEG) is an amphiphilic synthetic polymer which has shown favourable physical–chemical properties in the formulation of bioerodible polymeric nanostructured systems for the controlled release of high and low molecular weight active agents [24]. In the past, nanoparticles based on VAM41-PEG polymers have always been prepared by means of the *co*-precipitation technique, whereas in this context, a combined emulsion/solvent evaporation process is applied. The first step consisted in the development of a stable nanoemulsion by testing the suitability of different surfactants, such as Hypermer B246-E, Span 80, Nonylfenolethoxylat and Brij 72, together with the high electrolyte concentrations of the DSM containing water phase. The use of Hypermer-B246-E together with Norpar 12 as the oil phase gave the best results in terms of nanoparticle dimension and system stability against aggregation and sedimentation.

After preparation and purification, nanoparticles were dispersed in almond oil, chosen as the final dispersant due to its well known skin-friendly properties. Almond oil, together with oils obtained from other prunus kernels such as apricot, peach, plum and cherry, is commonly used for the preparation of cosmetics and pharmaceutical systems [27–29].

3.2. Nanoparticle characterization

After the miniemulsion/solvent evaporation process, the resulting nanoparticles were purified by means of centrifugation.

As reported in Table 2, the formulation yield increases as a function of salt content. Without salt in the formulation system no pellet was obtained during centrifugation, indicating that no solid nanoparticles were formed, whereas the maximum yield was observed with the highest salt concentration. These results are in agreement with literature data reporting a stabilizing effect of electrolytes in emulsion systems, since the rate of coarsening and coalescence of water droplets in water in oil emulsions is decreased in presence of electrolytes [30].

DSM loaded nanoparticles dispersed in almond oil were characterized by dynamic light scattering, yielding an average particle diameter of 220–350 nm (Table 3).

No linear correlation between salt content of the formulation and particle size could be observed. Furthermore, the particle diameter distribution seems not to be affected by changes in molar salt content in the initial nanoemulsion.

Nanoparticle salt content and release were estimated by analysing the increase of conductivity of electrolytic solutions generated by the presence of released DSM in water.

Concerning the nanoparticle salt content, known amounts of dry, purified nanoparticles were dissolved in water at alkaline pH

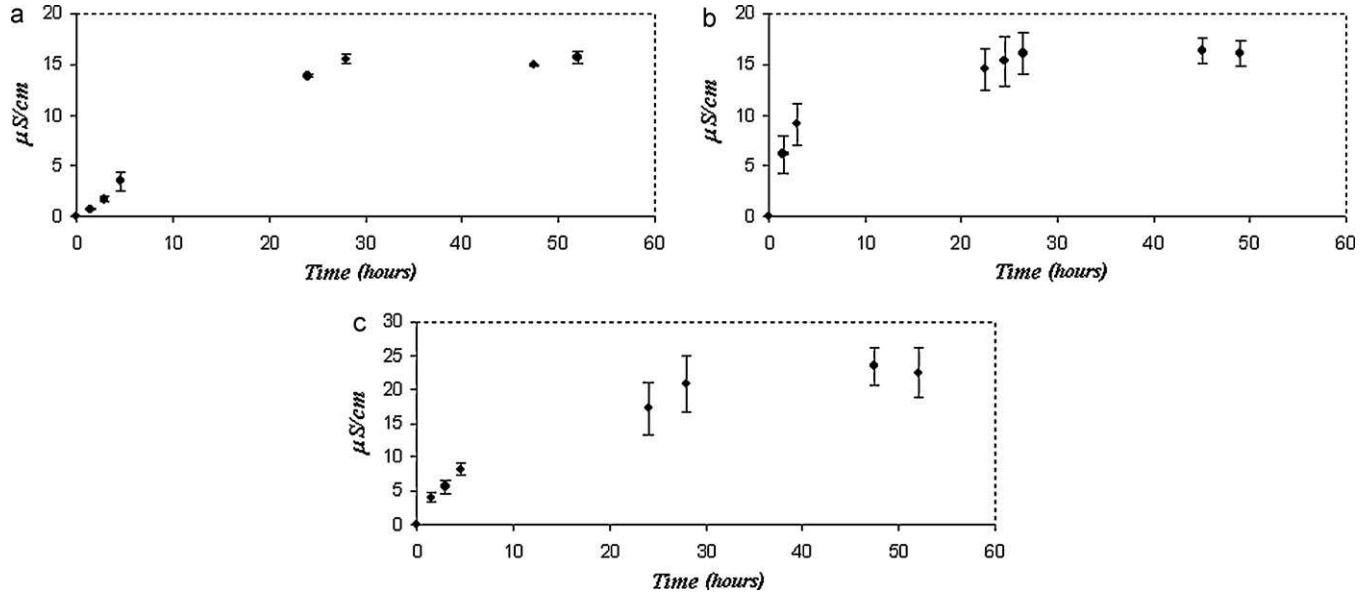

Fig. 2. Salt release profile of DSM loaded VAM41-PEG nanoparticles. (a) Nps_Dsm_½[A], (b) Nps_Dsm_[A], (c) Nps_Dsm_2[A].

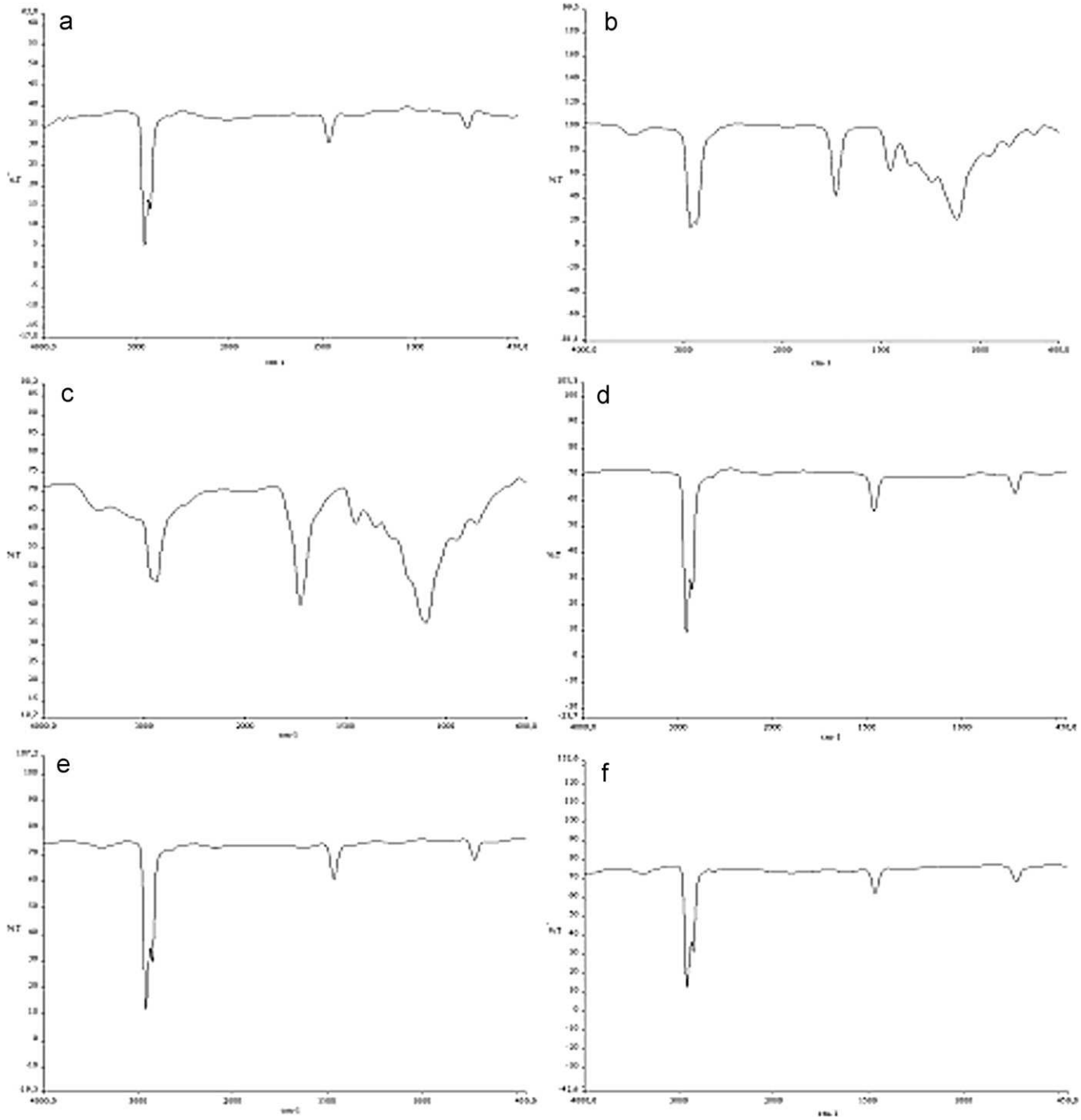

Fig. 3. FT-IR spectra analysis. DSM (A); Hypermer (B); VAM41-PEG (C); water samples from salt release kinetic experiments with Nps_Dsm_½[A] (D), Nps_Dsm_ [A] (E) and Nps_Dsm_2[A] (F).

(pH = 8) and the resulting solution was filled in a dialysis tube. The conductivity increase of the outer phase was correlated to the salt concentration by means of a calibration curve. The direct measurement of the conductivity of the nanoparticle solution was not applicable due to unknown contributions of polymer and surfactant to the total conductivity.

Nanoparticles loading and encapsulation efficiency (E.E.) values are reported in Table 4. The obtained results reveal a salt loading between 8 and 11.5 percent and an E.E. between 15 and 19.3 percent. However, no linear correlation between the salt concentration in the formulation system and the final loading of the polymeric nanoparticles could be observed. It can be concluded that despite the different DSM feeding, all the resulting nanoparticles possess similar properties regarding size and salt content. The amount of DSM present in the formulation system affected only the yield of the preparation process: higher salt concentration leads to more coagulation of the dissolved polymer into solid nanoparticles.

The salt release kinetic of the nanoparticles was monitored by suspending a known amount of dry, purified nanoparticles in almond oil. The resulting suspension was put on top of a known volume of water under mild stirring and the conductivity of the water phase was measured as a function of time. Pure almond oil

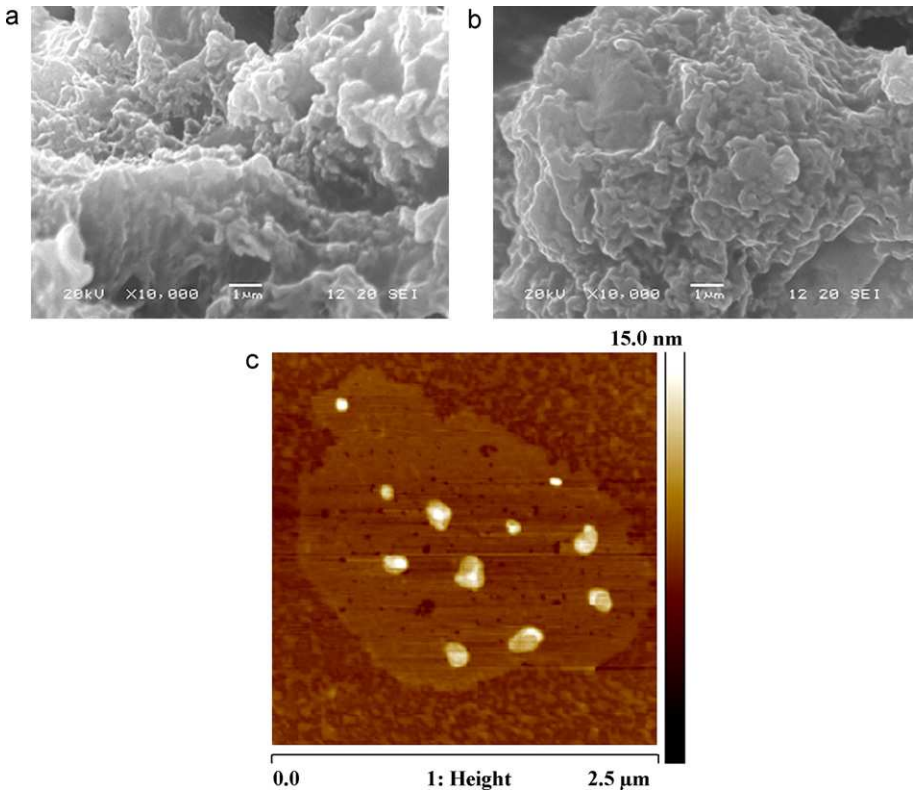

Fig. 4. SEM (a and b) and AFM (c) micrographs of VAM41-PEG based DSM loaded polymeric nanoparticles (Nps_Dsm_2[A]).

on top of water was used as a control sample. As reported in Fig. 2, a slow, progressive salt release from *Nps_Dsm_½[A]*, *Nps_Dsm_[A]* and *Nps_Dsm_2[A]* was observed, that reached a plateau after approximately 30 h in all of the three cases analyzed.

The above mentioned system was tuned as a model to analyse the nanoparticle's capability of releasing DSM across the oil–water interface, in order to obtain preliminary information regarding the suitability of the system to be used as a dermal drug delivery system.

In order to assess whether the increase of conductivity measured during the release kinetic experiments was only due to salt presence, FT-IR spectra analyses were performed. As reported in Fig. 3, FT-IR spectra analyses of VAM41-PEG polymer, surfactant, DSM and water samples from the release kinetic experiments were carried out.

Water samples from release experiments with *Nps_Dsm_½[A]*, *Nps_Dsm_[A]* and *Nps_Dsm_2[A]* formulations, showed FT-IR spectra which were completely super imposable to the DSM one. Since no characteristic peaks of polymer, surfactant and almond oil were detected in the water samples, it can be concluded that the conductivity increase was only due to a gradual and progressive salt release from the nanoparticle dispersions.

Since the Nps_Dsm_2[A] formulation gave the best results in terms of formulation yield, this preparation was selected to be

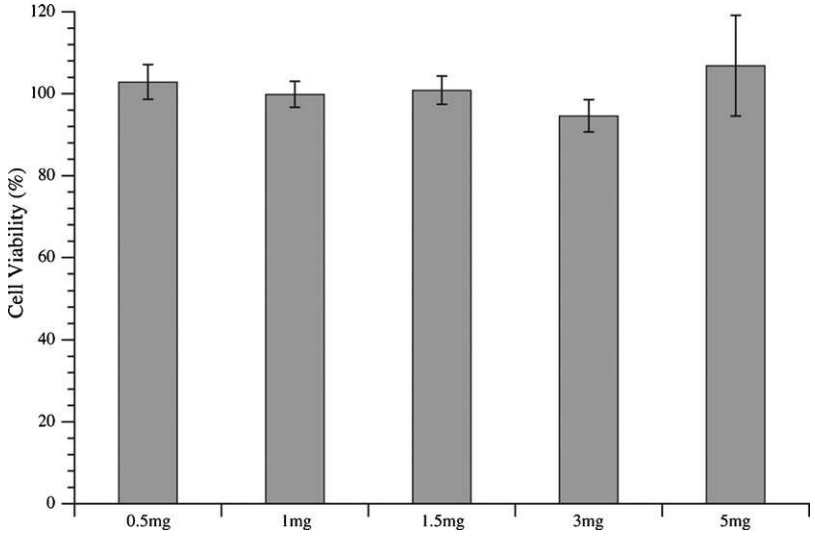

Fig. 5. WST-1 cytocompatibility test performed on DSM loaded polymeric nanoparticles (Nps_Dsm_2[A]).

investigated in terms of morphological features as well as biocompatibility properties.

To check the morphology, SEM and AFM analysis were carried out with dry, purified nanoparticles. As shown in Fig. 4, spherical nanoparticles can be detected in SEM samples, although it appears as if they were covered by a sticky layer. This can be attributed to a residual amount of paraffin oil which, apparently, was not completely removed during the centrifugation/diethyl ether washing step. These findings are also confirmed by AFM analysis which revealed the presence of solid nanometric structures, suggesting that the new developed combined miniemulsion/solvent evaporation technique leads to the preparation of nanostructured systems.

3.3. Nanoparticle cytocompatibility evaluation

To be considered suitable for biomedical applications, the nanoparticle formulation with best results in terms of size distribution and stability was submitted to a preliminary *in vitro* test to assess its biocompatibility. The cytocompatibility of Nps_Dsm_2[A] was evaluated using 3T3/BALB-C Clone A31 murine fibroblast as a cell line, as indicated by international ISO 10993 guidelines. Quantitative evaluation of cell viability performed by WST-1 assay indicates no toxicity for the developed Nps_Dsm_2[A] formulation; cell viability in presence of nanoparticles was comparable to the control cell profile up to a nanoparticle concentration of 5 mg/ml as shown in Fig. 5.

4. Conclusions

This work proposed a combined miniemulsion/solvent evaporation method for the production of DSM loaded VAM41-PEG based polymeric nanoparticles. The formulation process and conditions were optimised to obtain a uniform dispersion of nanoparticles in almond oil, possessing suitable features in terms of dimensions, morphology, salt release profile, and cytocompatibility.

Although further studies concerning the effectiveness of the therapeutic activity have to be performed, the results obtained in the present work indicated the potential of the developed system of being used as a pharmaceutical product for the topical treatment of skin diseases.

Acknowledgements

The present research was performed within the framework of the European Commission funded project “Skin-Treat” FP7 – NMP Theme under grant agreement n. 213202-2.

References

[1] J. Bhalerao, A.M. Bowcock, Hum. Mol. Genet. 7 (1998) 1537.
[2] A.M. Bowcock, J.N. Barker, Am. Acad. Dermatol. 49 (2003) 51.
[3] T. Nakatani, Y. Kaburagi, Y. Shimada, M. Inaoki, K. Takehara, N. Mukaida, S. Sato, J. Allergy Clin. Immunol. 107 (2001) 353–358.
[4] A. Garg, M.M. Chren, L.P. Sands, M.S. Matsui, K.D. Marenus, K.R. Feingold, P.M. Elias, Arch. Dermatol. 137 (2001) 53.
[5] T. Suetaki, S. Sasai, Y.X. Zhen, T. Ohi, H. Tazami, Arch. Dermatol. 132 (1996) 1453.
[6] M. Shahidullah, E.J. Ralffle, A.R. Rimmer, W. Frain-Bell, Br. J. Dermatol. 81 (1969) 722.
[7] T. Yoshiike, Y. Aikawa, J. Sindhvananda, J. Dermatol. Sci. 5 (1993) 92.
[8] Z. Felsher, S. Rothman, J. Invest. Dermatol. 6 (1945) 271.
[9] K.A. Grice, F.R. Bettley, Br. Med. J. 4 (1967) 195.
[10] A. Haratake, Y. Uchida, M. Schmuth, O. Tanno, R. Yasuda, J. Epstein, P.M. Elias, W.M. Holleran, J. Invest. Dermatol. 108 (1997) 769.
[11] D.J. Abels, Z. Even-Paz, D. Efron, Clin. Dermatol. 14 (1996) 653.
[12] E. Proksch, H.P. Nissen, M. Bremgartner, C. Urquhart, Int. J. Dermatol. 44 (2005) 151.
[13] M. Boaz, L. Shtendik, M. Oron, M. Portugal-Cohen, R. Kohen, A. Biro, R. Cernes, Z. Barnea, Z. Maor, Z. Katzir, Nephron. Clin. Pract. 113 (2009) 169.
[14] S. Halevy, H. Giryes, M. Friger, S. Sukenik, J. Eur. Acad. Dermatol. 9 (1997) 237.
[15] Z. Ma'or, Y. Henis, Y. Alon, E. Orlov, K.B. Sorensen, A. Oren, Int. J. Dermatol. 45 (2006) 504.
[16] A. Deters, E. Schnetz, M. Schmidt, A. Hensel, Forsch. Komp. Klas. Nat. 10 (2003) 19.
[17] M.P. Cohen, Y. Soroka, Z. Ma'or, M. Oron, T. Zioni, R. Neuman, R. Kohen, Y. Milner, Exp. Dermatol. 18 (2009) 781.
[18] H. Iizuka, K. Adachi, K.M. Halprin, V. Levine, J. Invest. Dermatol. 70 (1978) 250.
[19] K. Landfester, M. Willert, M. Antonietti, Macromolecules 33 (2000) 2370.
[20] J.M. Asua, Prog. Polym. Sci. 27 (2002) 1283.
[21] M. Antonietti, K. Landfester, Prog. Polym. Sci. 27 (2002) 689.
[22] C. Solans, P. Izquierdo, J. Nolla, N. Azemar, M.J. Garcia-Celma, Curr. Opin. Colloid. In. 10 (2005) 102.
[23] P. Izquierdo, J. Esquena, T.F. Tadros, J.C. Dederen, J. Feng, M.J. Garcia-Celma, N. Azemar, C. Solans, Langmuir 20 (2004) 6594.
[24] S. Hoellera, A. Spergera, C. Valenta, Int. J. Pharm. 370 (2009) 181.
[25] O.S. Aubrun, J.T. Simonnet, F.L. Alloret, Adv. Colloid Interface 108 (2004) 145.
[26] F. Chiellini, A.M. Piras, M. Gazzarri, C. Bartoli, M. Ferri, L. Paolini, E. Chiellini, Macromol. Biosci. 8 (2008) 516.
[27] G. Bernardo-Gil, C. Oneto, P. Antunes, F. Rodrigues, J.M. Empis, Eur. Food Res. Technol. 212 (2001) 170.
[28] A. Femenia, C. Rossello, A. Mulet, J. Canellas, J. Agric. Food Chem. 43 (1995) 356.
[29] K. Jovanovic, M. Milovanovic, J. Am. Oil. Chem. Soc. 70 (1993) 1101.
[30] M.P. Aronson, M.F. Petko, J. Colloid Interface Sci. 59 (1993) 134.